nature microbiology

BRIEF COMMUNICATION

DOI: 10.1038/s41564-017-0010-9

A microfluidics-based in situ chemotaxis assay to study the behaviour of aquatic microbial communities

Bennett S. Lambert[1,2,3], Jean-Baptiste Raina[4], Vicente I. Fernandez[1,2], Christian Rinke[5], Nachshon Siboni[4], Francesco Rubino[5], Philip Hugenholtz[5], Gene W. Tyson[5], Justin R. Seymour[4] and Roman Stocker[1,2*]

Microbial interactions influence the productivity and biogeochemistry of the ocean, yet they occur in miniscule volumes that cannot be sampled by traditional oceanographic techniques. To investigate the behaviours of marine microorganisms at spatially relevant scales, we engineered an in situ chemotaxis assay (ISCA) based on microfluidic technology. Here, we describe the fabrication, testing and first field results of the ISCA, demonstrating its value in accessing the microbial behaviours that shape marine ecosystems.

Planktonic microorganisms control the biogeochemistry and productivity of marine ecosystems[1]. This global-scale influence is governed by the rate at which individual microorganisms access organic substrates from the water column, which in turn is dependent upon the spatial distribution of substrates and the capacity of cells to exploit microscale nutrient hotspots[2]. Seawater is surprisingly heterogeneous at the scale of individual microorganisms[3], with nutrient hotspots on and around organic particles[4], phytoplankton cells[5] and zooplankton faecal pellets[6]. These microscale features of the water column represent important biogeochemical microenvironments where microbial activity and transformation rates considerably exceed background levels[5,7]. Consequently, the microbial behaviours involved in accessing and maintaining contact with these microenvironments can have profound implications for basin-scale chemical cycling, but have remained largely inaccessible by traditional oceanographic sampling approaches.

Chemotaxis—the ability of microorganisms to move in response to chemical gradients—is a pervasive microbial phenotype that allows them to exploit heterogeneous chemical landscapes. The first quantitative measurements of chemotaxis were carried out 50 years ago using the capillary assay[8], which relies on the molecular diffusion of a chemical cue from the tip of a capillary tube to attract bacteria. Many alternative techniques have since been developed[9], including the recent application of microfluidics to establish controlled chemical gradients and quantify microbial responses[10]. Although chemotaxis is conventionally studied in the context of physically structured microenvironments such as biofilms, or in association with animal or plant hosts[11], there is growing evidence (albeit mostly limited to laboratory-based assays[12]) that indicates its ubiquity among copiotrophic planktonic marine microorganisms[3,5], which probably use it to access fleeting microscale nutrient patches in the water column[1,3]. To quantify and understand the importance of chemotaxis in the ocean, we need to measure this behaviour in situ. Here, we leverage the control afforded by modern microfabrication methods to design an in situ chemotaxis assay (ISCA) that enables measurement of marine microbial behaviour under natural conditions.

The ISCA is a robust and rapidly producible device that bridges the gap between laboratory-based microfluidics and traditional oceanographic methods, by providing an in situ system to interrogate microbial behaviour (Fig. 1). The ISCA consists of a scalable array of 110 µl wells embedded in a polydimethylsiloxane (PDMS) slab, with each well connected to the outside seawater by a port (0.8 mm diameter, 1.6 mm depth) (Fig. 1a and Supplementary Fig. 1; see Methods). The device is made of inert materials, is single-use and is fabricated using a standard soft lithography workflow, based on a mould created using three-dimensional printing. Each well is filled with a chemoattractant, which diffuses out of the port and into the surrounding seawater during deployment, resulting in a chemical microplume extending 1–2 mm above each well (Supplementary Video 1). As in the capillary assay, microorganisms can respond to a specific cue by using chemotaxis to swim into the well. Following deployment, cells can be enumerated with flow cytometry to quantify the strength of chemotactic accumulation within each well and DNA sequencing approaches applied to identify responding microbial populations.

Before field deployment, we thoroughly tested the ISCA in the laboratory by employing several chemotactic bacterial isolates to assess the potentially confounding roles of random motility, ambient flow and Brownian motion. To measure the chemotactic accumulation dynamics of bacteria within individual wells, a small ISCA (2 × 2 array of wells) was embedded within a microcosm placed on the stage of an inverted microscope (Supplementary Fig. 1). The microcosm contained fluorescently labelled *Vibrio coralliilyticus* (YB2), a copiotrophic marine bacterium and coral pathogen[13], suspended in 0.22-µm-filtered artificial seawater (Instant Ocean, Spectrum Brands). Bacterial fluorescence was used to identify cells throughout the well depth by epifluorescence microscopy. One ISCA well

[1]Department of Civil and Environmental Engineering, Ralph M. Parsons Laboratory, Massachusetts Institute of Technology, Cambridge, MA 02139, USA. [2]Department of Civil, Environmental and Geomatic Engineering, Institute for Environmental Engineering, ETH Zurich, 8093 Zurich, Switzerland. [3]Department of Applied Ocean Physics and Engineering, Woods Hole Oceanographic Institution, Woods Hole, MA 02543, USA. [4]Climate Change Cluster, University of Technology Sydney, Ultimo 2007 NSW, Australia. [5]Australian Centre for Ecogenomics, School of Chemistry and Molecular Biosciences, The University of Queensland, St. Lucia 4072 QLD, Australia. Bennett S. Lambert and Jean-Baptiste Raina contributed equally to this work. *e-mail: romanstocker@ethz.ch

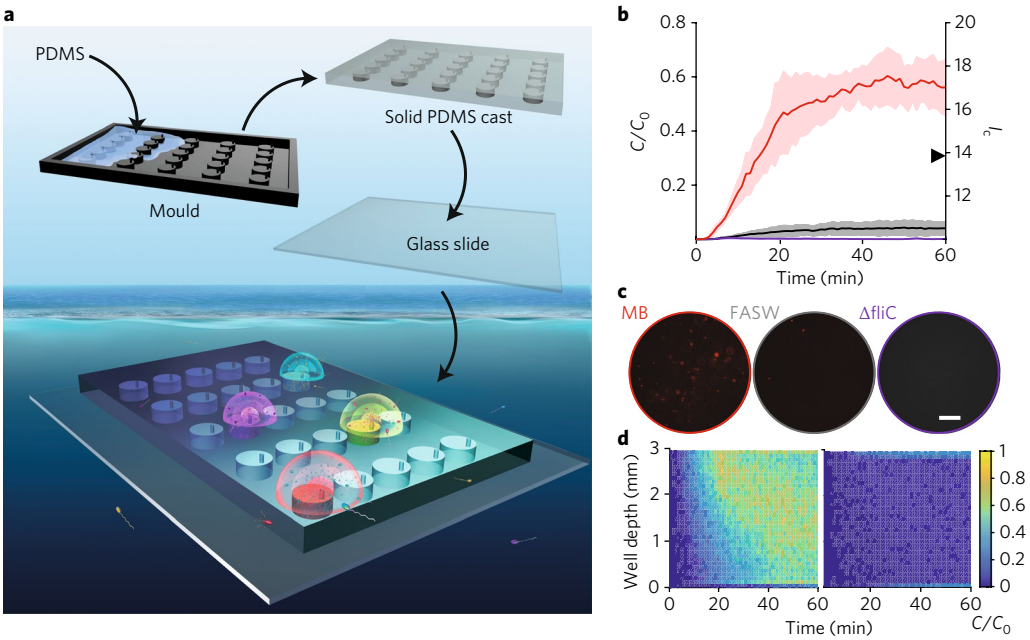

Fig. 1 | Fabrication of the in situ chemotaxis assay (ISCA) and laboratory tests. a, Polydimethylsiloxane (PDMS) is cast onto a 3D printed mould and cured overnight. The solid PDMS, containing multiple wells, is then excised and plasma-bonded onto a glass slide (100 mm × 76 mm × 1 mm). Each well has an independent connection to the external environment via a port, through which chemicals can diffuse and microorganisms enter. Upon deployment, the ISCA produces chemical microplumes that mimic transient nutrient patches. Chemotactic bacteria respond by swimming into the wells of the device and after collection can be enumerated by flow cytometry and identified by sequencing. Computer-aided design files are provided in Supplementary File 1. **b**, Accumulation of fluorescently labelled marine isolates within ISCA wells in a laboratory microcosm quantified through video microscopy. The solid line represents the mean cell concentration ($n = 3$) over the imaging volume normalized to that in the surrounding medium and the shaded area is one standard deviation around the mean. Red: *V. coralliilyticus* swimming into a well initially filled with 10% Marine Broth (MB). Black: *V. coralliilyticus* and filtered artificial seawater (FASW, control). Purple: *M. adhaerens* non-motile mutant control (ΔfliC) and FASW (non-motile control; almost indistinguishable from zero). The triangle on the right-hand axis indicates the chemotactic index, I_c, for *V. coralliilyticus* after 60 min, calculated as the ratio of the number of cells responding to the chemoattractant and to the FASW. **c**, Representative images taken at mid-depth of the well after 60 min. Scale bar, 100 μm; $n = 3$. Note the near absence of cells from the controls (FASW and ΔfliC). **d**, Average accumulation through well depth and time of fluorescently labelled *V. coralliilyticus* in response to 10% Marine Broth (left, $n = 3$) and in response to FASW (right, $n = 3$). Minor accumulation shows that random motility does not contribute significantly to the final concentration of cells in each well. The colour bar applies to both panels and indicates the concentration of cells, C, in each image, normalized to that in the surrounding medium, C_0. The resolution is 80 μm in depth and 1 min in time.

was filled with a broad-spectrum chemoattractant (Marine Broth, Becton Dickinson) and another, serving as negative control, with filtered artificial seawater (see Methods; Supplementary Fig. 2). We used 10% Marine Broth inside the ISCA to generate signals at ecologically relevant concentrations (Supplementary Note 2). We imaged a predetermined location within each well, scanned over the entire well depth every minute for 60 min, and used image analysis to obtain cell counts as a function of time (see Methods).

The ISCA captured the characteristically strong chemotactic response of *V. coralliilyticus*[13]. An intense accumulation of cells occurred within wells containing Marine Broth (56.1 ± 10.4% of the microcosm cell density; $n = 3$), whereas the accumulation was negligible in the control wells (4.1 ± 2.4% of the microcosm cell density; $n = 3$). The ratio of the cell concentrations in treatment and control wells—the chemotactic index (I_c, the ratio of cells in treatment to cells in control)—was 14, denoting a strong response to the chemoattractant (Fig. 1b and Supplementary Figs. 3 and 4). These results confirm that the ISCA generated robust chemical signals and effectively attracted and retained chemotactic bacteria in the wells (Fig. 1c). The high value of I_c also indicates that random motility—which results in bacteria entering wells even in the absence of chemical gradients—is negligible compared to chemotaxis. Furthermore, experiments with a non-motile bacterium, *Marinobacter adhaerens* (HP15 ΔfliC), did not result in significant cell accumulation relative to the surrounding medium (0.09 ± 0.03% of the microcosm cell density; $n = 3$; Fig. 1b and Supplementary Fig. 5), implying that environmental factors such as fluid flow do not contribute significantly to the accumulation of cells in the wells under laboratory conditions.

Imaging-based laboratory experiments revealed three phases in the chemotactic accumulation: (1) an initial lag phase lasting ~5 min, where cells swam into the inlet port but had not yet entered the main cavity of the well; (2) a sharp increase in bacterial abundance in the well as bacteria began to enter, lasting until ~25 min; and (3) a slowdown in the accumulation (at 30–40 min) as the outward diffusive flux of cells began to balance the inward chemotactic flux (Fig. 1b). In the second phase, the spreading of cells from the top of the well downwards (Fig. 1d and Supplementary Figs. 3 and 6) provides direct visual evidence of the chemotactic dynamics and helps rule out confounding factors such as residual fluid flow in the wells.

To further validate the ISCA, we compared the observed accumulation dynamics with those predicted by a mathematical model of chemotaxis (see Methods; Supplementary File 2, Supplementary Videos 1 and 2 and Supplementary Figs. 6–9). Chemotactic transport models are only well developed for a few specific model organisms such as *Escherichia coli*[14], so the model was parameterized for *E. coli* responding to the non-metabolizable chemoattractant α-methylaspartate, a pairing studied extensively in the chemotaxis literature[15]. To allow direct comparison, a laboratory ISCA experiment was

carried out with a fluorescent strain of *E. coli* (AW405) and α-methylaspartate as the chemoattractant (see Methods; Supplementary Fig. 6). In this experiment, image stacks over the entire well's depth were acquired over time at two different locations, one close to the port (1.5 mm from the edge of the inlet) and the second further away (2.5 mm), so that the progression of chemotactic bacteria within the well could be followed. The comparison of experimental results with model predictions demonstrated highly consistent timescales and magnitudes of accumulation, with cells first appearing in the field of view at ~10 min (1.5 mm location) and ~20 min (2.5 mm location) (Supplementary Fig. 9). Furthermore, the chemotactic drift velocity inferred from the time lag between the appearance of bacteria at the two imaging locations (~1.1–1.85 μm s^{-1}; $n=3$) is consistent with values reported in the literature for *E. coli*[16], further supporting the absence of residual flows within the device. This set of experiments in conjunction with the numerical model confirms that chemotaxis is the primary mode of accumulation in the ISCA.

With experimental results providing confidence in the ISCA's operation, the device was next tested in situ. We deployed four replicate ISCAs (each consisting of a 5×5 array of wells) for 1 h (a duration well below the typical doubling times of marine microorganisms[17]; Supplementary Note 3) in surface waters (1 m depth) at a coastal marine site in Sydney, Australia (Clovelly Beach, 33.91°S, 151.26°E). To retain consistency with the laboratory-based experiments, we compared the chemotactic response of microorganisms to wells filled with Marine Broth and to control wells filled with filtered seawater (0.02 μm; see Methods) derived from the deployment site. To avoid density differences between well contents and bulk seawater, which could lead to density-driven flows, this filtered seawater was also used to dilute the Marine Broth.

Although fluid flow into the wells was ruled out in the laboratory experiments, in situ conditions are far more dynamic and may potentially disrupt the chemical microplumes emanating from the wells. To prevent this, each ISCA was mounted within a transparent 1.9 l volume, laser-cut acrylic enclosure (Supplementary Fig. 10). The enclosure was soaked for 48 h in ddH_2O to remove labile dissolved organic matter from the acrylic surface. The stable environment provided by the enclosure also ensured that bacteria were not swept past the wells at a speed that overpowered their swimming ability. This replicates the physical environment that cells encounter at the microscale, where bacteria and nutrient hotspots are essentially transported together and movement of one relative to the other is primarily achieved through motility[18]. After securing the ISCA, the acrylic enclosure was slowly filled with seawater while being submerged, and, once at its final depth, was completely sealed using a plug and left in situ for 1 h (Supplementary Fig. 11). Strong chemotaxis was observed, with the mean number of bacteria in Marine Broth wells 3.6±0.2 times greater than in negative control wells (*t*-test, $n=4$, $P<0.005$; Fig. 2). These results constitute in situ confirmation that pelagic marine bacteria exhibit strong chemotaxis, which not only supports the results of previous laboratory-based studies[3,5,19], but also long-standing hypotheses about the occurrence of this behaviour in the pelagic environment[1,2,20].

Chemotactic populations were identified by their 16S rRNA sequences in shotgun metagenomic data obtained using a low-input DNA library preparation procedure[21]. Whereas the taxonomic profile of bulk seawater at the sampling site was characteristic of a typical coastal marine community, including a high proportion of non-motile Pelagibacteraceae (Fig. 2), the ISCA wells containing Marine Broth were highly enriched with motile copiotrophs, including Vibrionales and Alteromonadales (Supplementary Fig. 12). These groups are well known for their chemotactic capabilities[5] and metabolic versatility[22], enabling them to respond to and use a large number of organic compounds, such as those present in Marine Broth. These results therefore provide in situ confirmation that copiotrophic microorganisms can rapidly respond to

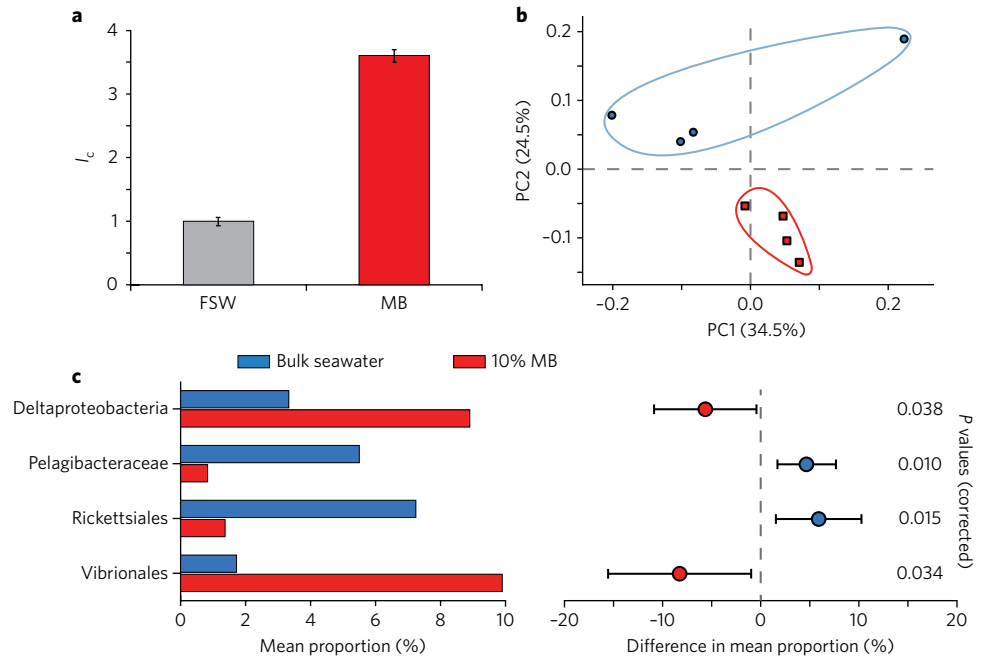

Fig. 2 | Field tests of the ISCA. a, Chemotactic index I_c, denoting the concentration of cells within ISCA wells, normalized by the mean concentration of cells ($n=4$) within wells containing filtered seawater (FSW), after 60 min field deployment. Cells were enumerated by flow cytometry (MB: 9.4±0.4×10^3; FSW: 2.6±0.3×10^3 cells ml^{-1}). Note that wells containing 10% MB had significantly more bacteria than the FSW control (*t*-test, $n=4$, $P<0.005$). Error bars represent standard errors. **b**, Principal component analysis comparing family-level taxonomic profiles of bulk seawater from the sampling site with the contents sampled from the ISCA wells containing MB. **c**, Taxa differing significantly between bulk seawater and ISCA wells containing MB ($n=4$). *P* values were corrected for multiple hypothesis testing using the Bonferroni correction (95% confidence intervals).

microscale nutrient patches[19]. In addition, less-studied motile taxa, such as Flammeovirgaceae, were also enriched in the wells containing Marine Broth (Supplementary Fig. 12). The latter finding reveals the power of the ISCA to identify cryptic chemotactic taxa and highlights its potential use in prospecting for taxa capable of responding to specific chemicals, such as pollutants.

We believe that the ISCA represents a significant advance in microbial oceanography, enabling interrogation of the chemically mediated interactions that support the base of the food web and drive biogeochemical cycles at scales relevant to microorganisms in their natural environment. Here, we capitalized on rapid advances made in the fields of microfluidics and low-input DNA sequencing[21] to couple micro-engineering with genomic analyses. The ISCA is not only deployable in aquatic environments, but also in any system containing a liquid phase (for example, soil and sediment matrices or wastewater systems). Future use of the device will enable high-throughput testing of environmentally derived chemicals and, when coupled with genomic and metabolomic analyses, will generate rich data sets allowing the behaviour and chemical ecology of microorganisms to be dissected within their natural habitats.

Methods

ISCA design and assembly. A 3D printed mould was designed using SolidWorks 2015 (Dassault Systemes SolidWorks) and made out of the polymer VeroGrey on an Objet30 3D printer (Stratasys; Supplementary File 1). In the implementation used for the field deployments, each ISCA consisted of an array of 5 × 5 wells. Each well was 6.8 mm in diameter and 3 mm in depth, which corresponds to ~110 µl of fluid (Supplementary Fig. 1), a volume selected based on the estimated lower limit of input required for DNA extraction and sequencing. The wells were spaced 17 mm apart between rows (centre to centre) and 9 mm within a row (Supplementary Fig. 1). The port of each well was offset from the centre of the well to allow release of air bubbles during filling of the well (Supplementary Fig. 1). Considering a representative diffusion coefficient D of 1×10^{-9} m s^{-1}, the estimated distance L a solute travels in a time $t = 1$ h is $L = \sqrt{4Dt} = 3.8$ mm. The spacing used therefore ensures no well-to-well interaction of the chemical plumes within typical deployment times of 1 h. The port diameter was 800 µm with a depth of 1.6 mm (Supplementary Fig. 1). A high aspect ratio for the inlet port was selected to diminish the effects of cavity flow on device performance (Supplementary Note 1).

Each mould was filled with 26 g of polydimethylsiloxane (PDMS; 10:1 PDMS base to curing agent, wt/wt; Sylgard 184, Dow Corning). Curing was carried out overnight at 40 °C (the deflection point of VeroGrey is 48 °C). The cured PDMS slab (95 mm × 65 mm × 4.6 mm) was cut using a razor blade and carefully peeled from the mould. The PDMS blocks were inspected and any port obstructions cleared using a biopsy punch of the appropriate diameter (ProSciTech). Finally, the devices were UV-sterilized and plasma-bonded to sterile glass microscope slides (100 mm × 76 mm × 1 mm, VWR) by exposing both to oxygen plasma for 5 min using a plasma cleaner/sterilizer (Harrick Scientific). Following bonding, the ISCA was heated at 90 °C for 10 min to accelerate the formation of covalent bonds and then stored at room temperature until use.

Laboratory experiments. *Bacterial cultures.* The marine bacterium *V. coralliilyticus* (YB2) was used as a model organism for laboratory experiments due to its high level of motility and strong chemotactic response[13]. A glycerol stock of *V. coralliilyticus* was streaked onto Difco 2216 Marine Broth (BD Biosciences) agar plates containing 50 µg ml^{-1} kanamycin (Axonlab). Individual colonies were then removed and grown in 1% (vol/vol) 2216 Marine Broth in 0.22-µm-filtered artificial seawater (Instant Ocean, Spectrum Brands) for 22 h (ref. [13]). The cultures were then diluted 1/20 (vol/vol) in 0.22-µm-filtered Instant Ocean to obtain the bacterial suspension used in the experiments. All cells were grown at 30 °C and 180 r.p.m.

To ensure that bacteria found in the ISCA well had entered via chemotaxis and not by flushing due to fluid flow or Brownian motion, we carried out an experiment with non-motile bacteria. We used *M. adhaerens* (HP15 ΔfliC), a non-motile mutant lacking fliC, a gene necessary for flagellar synthesis[23]. A glycerol stock of *M. adhaerens* HP15 ΔfliC was streaked onto Difco 2216 Marine Broth agar plates containing 50 µg ml^{-1} ampicillin (Axonlab). Individual colonies were then suspended in 10% 2216 Marine Broth for 1 day. The cells were then washed three times in 0.22-µm-filtered Instant Ocean before being diluted 1/10 (vol/vol) in 0.22-µm-filtered Instant Ocean to obtain the bacterial suspension used in the experiments. All cells were grown at 30 °C and 180 r.p.m.

To directly compare experimental results to results from the mathematical model of chemotaxis, which was implemented based on parameters for *E. coli* chemotaxis (due to the lack of information on parameters for marine bacterial chemotaxis), we also performed laboratory experiments with *E. coli* (AW405). To directly visualize the bacteria in the ISCA wells, *E. coli* were transformed to carry a plasmid constitutively expressing a red fluorescent protein (pFM210)[24,25]. Cells in log phase (optical density (OD) = 0.3) were washed and resuspended in 50 mM calcium chloride, heat-shocked in a solution containing plasmid DNA, and spread on tryptone broth plates containing 50 µg ml^{-1} kanamycin. Resistant colonies were regrown in tryptone broth containing 50 µg ml^{-1} kanamycin and screened for fluorescence. Glycerol stocks (15% vol/vol) of colonies displaying strong fluorescent signal were made and stored at −80 °C. The transformed *E. coli* were streaked onto tryptone broth agar plates containing 50 µg ml^{-1} kanamycin. Individual colonies were then removed and grown overnight in tryptone broth containing 50 µg ml^{-1} kanamycin. These cells were then diluted 1:100 in tryptone broth and incubated until they reached mid-exponential phase (OD = 0.3). Cells were then diluted 1/20 (vol/vol) in 0.22-µm-filtered motility medium (10 mM potassium phosphate, 0.1 mM EDTA, 1 µM methionine, 10 mM lactic acid, pH 7) to obtain the suspension used in the experiments. All cells were grown at 30 °C and 180 r.p.m.

Assembly of the integrated ISCA for laboratory experiments and chemotaxis experiments with isolates. To visualize chemotactic accumulations in the ISCA wells without interference by external fluid flows, a modified version of the ISCA was integrated into a microcosm designed for use on an inverted microscope. To achieve this, an ISCA was prepared in the same manner as described above, but only four of the wells were excised from the PDMS block to reduce the footprint of the device (Supplementary Fig. 1). The four wells were plasma-bonded to the centre of a microscope slide (75 mm × 50 mm × 1 mm) and a four-walled PDMS enclosure was plasma-bonded around the wells (Supplementary Fig. 1). The design of the mould used to generate the enclosure is provided in Supplementary File 1. This ISCA-containing microcosm was placed onto the stage of an inverted microscope (Eclipse Ti-E, Nikon). A well of the integrated ISCA was filled with the prepared bacterial suspension and three stacks of images (80 µm step size, 2,960 µm total) were acquired within this well to calculate the bacterial concentration throughout the microcosm. This bacterial concentration (C_0) was subsequently used to normalize the concentration measured in individual treatments, so that chemotactic accumulations were quantified relative to the absolute concentration of bacteria present in each experiment. The device was then removed from the microscope stage and one well of the device was filled with a chemoattractant (10% Marine Broth for experiments with *V. coralliilyticus*; 100 µM α-methylaspartate for experiments with *E. coli*; Supplementary Figs. 3 and 6), while a second well was filled with filtered artificial seawater (FASW) for experiments with *M. adhaerens and V. coralliilyticus* or with motility medium for experiments with *E. coli*, both serving as negative controls (Supplementary Figs. 4 and 7). After placing the microcosm back on the microscope stage, an initial image stack was acquired (80 µm step size, 2,960 µm total; time $t = 0$). The microcosm was then filled with the bacterial suspension and one image stack was acquired every minute for 60 min (Supplementary Fig. 2). Image stacks acquired within the wells consisted of one image for every 80 µm of depth, throughout the depth (2,960 µm) of the well. Image acquisition was carried out with a 20x objective using Nikon Elements software and a Zyla 4.2 PLUS sCMOS camera (Andor).

Image analysis. To quantify cells in our laboratory experiments it was necessary to accurately identify cells in each image, while excluding out-of-focus cells and debris. To accomplish this, image processing and analysis were carried out in MATLAB 2015a (MathWorks) using the Image Processing Toolbox. The image stacks obtained in Nikon Elements were first filtered with a bandpass Gaussian filter to reduce high-frequency noise and remove larger objects due to uneven illumination or out-of-focus halos. The processed images were then segmented to identify candidate bacteria. These candidates were subsequently gated based on average pixel intensity and object area to enumerate the cells in each image. The resulting cell counts were manually verified for a subset of images in each image stack. Videos demonstrating the success of the image analysis in identifying cells are provided in Supplementary Videos 5–7. The analysis was successful in identifying the majority of cells while excluding out-of-focus cells.

To determine absolute cell concentrations it was necessary to quantify the depth of field for each of the three strains of bacteria used, so that the cell concentration could be computed from the number of cells and the imaging volume. The detection of cells described above depends on the choice of gating parameters and the fluorescent intensity of the cells themselves. The depth of field was determined empirically by analysis of vertical image stacks of fluorescently labelled cells on a horizontal surface. The image processing described above was carried out and the depth of field was defined as twice the height at which the number of detected in-focus cells was <10% of the value at the surface. This depth of field was then used consistently throughout the analysis to determine cell concentrations. The cell concentration in each well (C) was normalized by the cell concentration in the initial bacterial suspension (C_0) measured in a well filled with that suspension.

Mathematical model of chemotaxis into ISCA wells. We compared our laboratory observations with the predictions from a mathematical model, implemented in COMSOL Multiphysics 5.1 (COMSOL) using the 'Transport of Diluted Species' and 'Coefficient Form PDE' modules. The model domain

consisted of a single three-dimensional ISCA well and the fluid (1 ml) outside the inlet port (Supplementary Fig. 8). The model, based on coupled partial differential equations, solves for the spatiotemporal distribution of the chemoattractant (Supplementary Video 1), which is then used as input into a transport equation for populations of chemotactic or non-chemotactic bacteria, modelled as a concentration of cells[26] (Supplementary Video 2 and Supplementary Fig. 9). The mesh consisted of two domains (port and well, Supplementary Fig. 8) and boundary layers were enabled, with edges trimmed. The chemical field and bacterial field were initialized as opposing smoothed step functions, with the transition zone determined by the penetration depth of a cavity flow (Supplementary Note 1). Because chemotactic transport models are only well-developed for specific model organisms and in particular *E. coli*[14], the model was parameterized for *E. coli* responding to the non-metabolizable chemoattractant α-methylaspartate, based on a model described previously[16]. The model was initialized with the bulk fluid containing 1×10^5 cells ml^{-1} and the well contained 100 µM α-methylaspartate. The model then ran in two stages: an initial 1 s stage with 0.1 s time steps, and a subsequent 1 h stage with 10 s time steps. This two-stage method saves on computation time while allowing sufficient temporal resolution early in time, when very steep gradients occur. The output of the model consisted of the concentration of chemoattractant and bacteria over the full computational domain and over time, which was then used to compare with experimental observations. The COMSOL model file is provided in the Supplementary Information (Supplementary File 2).

Field deployments. Field deployments took place in April 2016 at Clovelly Beach (33.91°S, 151.26°E), located on the eastern coast of Australia. To ensure the initial absence of microbial cells in the seawater used as both a negative control and as a base for chemoattractant suspensions, seawater from the site was subjected to a triple-filtration process, where 50 ml was collected and first filtered through a 0.2 µm Sterivex filter (Millipore), followed by a 0.2 µm Millex FG (Millipore) and finally through a 0.02 µm Anotop filter (Whatman). Five 80 µl samples of this ultrafiltered seawater were fixed in 2% glutaraldehyde for subsequent flow cytometry analysis, which confirmed the effectiveness of this filtration protocol in removing all bacterial cells.

For initial testing of the ISCA in the field we used a broad-spectrum chemoattractant, Marine Broth 2216 (Beckton Dickson), a common growth medium for marine microorganisms. A 10% final concentration of Marine Broth was resuspended in freshly ultrafiltered seawater from the deployment site immediately before loading in the ISCA wells. The ISCA wells were filled with the port facing up: sterile 1 ml syringes and 27G needles (Terumo) were used to load samples into the wells. The diameter of the needle being smaller than the port allowed air to escape as the well was filled. This procedure was found to be optimal in ensuring complete filling, with no residual air bubbles in the wells.

Across each ISCA, treatments (filtered seawater or Marine Broth) were randomly allocated to an ISCA row (consisting of five wells). All wells in a row acted as technical replicates and four different ISCAs were deployed in parallel to act as biological replicates. Each ISCA was secured inside a deployment enclosure (Supplementary Fig. 10), which was sealed by pressure-sensitive tape (Scotch, 3M) and an enclosure plug to seal the bottom drain (Supplementary Fig. 11). Each enclosure was then attached to a modified vice enabling the deployed ISCA to be firmly secured to a rigid structure (for example, pontoon, ladder or pole) to minimize enclosure movement and standardize the deployment depth at 1 m. As the enclosures were submerged, they slowly filled with seawater through the enclosure inlets. Once completely filled with seawater, the enclosure inlets were plugged (to seal the enclosure) and the ISCAs were left in situ for 1 h.

Upon retrieval of the enclosures, the side outlets were unsealed progressively to slowly drain the seawater. Once the enclosures were completely empty, the contents of ISCA wells were then collected using 1 ml syringes and 27G needles (Terumo), with the ports facing down. For each ISCA, the liquid in the wells acting as technical replicates was pooled (five wells per treatment) to increase the amount of DNA collected per sample. The total volume of each pooled sample was 550 µl, of which 80 µl was fixed with filtered glutaraldehyde (2% final concentration) for flow cytometry analysis (conducted on fresh samples the same day) and 470 µl was snap-frozen immediately in liquid nitrogen for subsequent DNA extraction and sequencing. In addition to the ISCA samples, bulk seawater samples ($n=4$) were also collected for both flow cytometry and DNA sequencing. Water temperature and salinity were recorded with a multiprobe meter (WTW Multiparameter Meter, WTW).

Although the deployment enclosure was required to generate a microenvironment that is analogous to that experienced by planktonic bacteria interacting with chemical hotspots in the water column, the manner in which the ISCA is housed is entirely dependent on the scientific question investigated. One may wish to study the interaction of bacteria with cues released from surfaces, such as in the benthic environment. In this case, the surface is stationary but the bacteria are advected by the flow, a scenario that is best replicated by deploying the ISCA without an enclosure.

Molecular analysis. Samples for flow cytometry were transferred into sterile Titertube micro test tubes (Bio-Rad), stained with SYBR Green I (ThermoFisher), incubated for 15 min in the dark and analysed on a BD Accuri C6 flow cytometer (Becton Dickinson) with filtered MilliQ water as the sheath fluid. For each sample, forward scatter (FSC), side scatter (SSC), green (SYBR Green) and red (chlorophyll) fluorescence were recorded. The samples were analysed at a flow rate of 35 µl min^{-1}. Microbial populations were characterized according to SSC and SYBR Green fluorescence[27] and cell abundances were calculated by running a standardized volume of sample (50 µl). To quantify the strength of chemotaxis, the chemotactic index I_c was calculated by dividing the number of cells present in the chemoattractant treatment by the number of cells present in the filtered seawater negative control.

DNA extraction, library preparation, sequencing and bioinformatics. DNA extraction from seawater samples was performed using the UltraClean Tissue & Cells DNA Isolation Kit, following the manufacturer's instructions with minor modifications, as described previously[21]. Libraries for shotgun metagenomic sequencing were prepared using the Nextera XT DNA Sample Preparation Kit (Illumina) following a previously described modified protocol designed for generating low-input DNA libraries[21]. All libraries were sequenced with an Illumina NextSeq 500 platform 2× with 150 bp High Output v.1 run chemistry. Libraries were pooled on an indexed shared sequencing run, resulting in 1/37 of a run or ~3.2 Gbp per sample. The raw fastq read files were deposited on the Microscale Ocean webpage (http://microscaleocean.org/data/category/12-in-situ-chemotaxis-assay).

To characterize the composition of bacterial communities, 16S rRNA gene-based taxonomic profiles of the samples were generated with GraftM (http://geronimp.github.io/graftM) using the 16S rRNA package (4.39.2013_08_greengenes_97_otus.better_tree.gpkg). The pipeline was designed to identify reads encoding 16S rRNA genes based on hidden Markov models and to assign taxonomic classifications by comparison against a reference taxonomy. A detailed feature description, user manual and example runs are available on the GitHub wiki (https://github.com/geronimp/graftM/wiki). For the heatmap, the GraftM output was manually curated, whereby mitochondrial and chloroplast sequences were removed. Relative abundances were calculated and trimmed (>5%) in the software environment R (www.r-project.org) and the data were displayed as a heatmap (pheatmap). Differences in 16S rRNA gene abundance between samples ($n=4$) were compared via analysis of variance (ANOVA), using the Statistical Analysis of Metagenomic Profiles (STAMP) software[28].

In addition, a reference genome-based taxonomic classification approach was used based on the bacterial genome collection in GTDB (gtdb.ecogenomic.org). Reads were aligned back with Bowtie2 (ref. [29]), BAM files were created and reads counted with SAMtools[30]. Taxonomy parsing and cross-reference of sequences were performed using MGKit (bitbucket.org/setsuna80/mgkit) and analysis was performed in Python (www.python.org) and Pandas (pandas.pydata.org/) environments. Counts were grouped to the class level and relative abundances calculated. Taxonomic assignments that accounted for <5% of the total reads were filtered and a clustered heatmap created with Seaborn (http://seaborn.pydata.org/index.html).

Data availability. The raw fastq read files are available on the Microscale Ocean webpage (http://microscaleocean.org/data/category/12-in-situ-chemotaxis-assay). The experimental image data are available from the corresponding author upon request (due to the large file sizes).

Received: 10 June 2017; Accepted: 19 July 2017;
Published online: 28 August 2017

References

1. Azam, F. Microbial control of oceanic carbon flux: the plot thickens. *Science* **280**, 694–696 (1998).
2. Azam, F. & Malfatti, F. Microbial structuring of marine ecosystems. *Nat. Rev. Microbiol.* **5**, 782–791 (2007).
3. Blackburn, N., Fenchel, T. & Mitchell, J. Microscale nutrient patches in planktonic habitats shown by chemotactic bacteria. *Science* **282**, 2254–2256 (1998).
4. Kiørboe, T., Grossart, H.-P., Ploug, H. & Tang, K. Mechanisms and rates of bacterial colonization of sinking aggregates. *Appl. Environ. Microbiol.* **68**, 3996–4006 (2002).
5. Smriga, S., Fernandez, V. I., Mitchell, J. G. & Stocker, R. Chemotaxis toward phytoplankton drives organic matter partitioning among marine bacteria. *Proc. Natl Acad. Sci. USA* **113**, 1576–1581 (2016).
6. Jefferson, T. T. Zooplankton fecal pellets, marine snow and sinking phytoplankton blooms. *Aquat. Microb. Ecol.* **27**, 57–102 (2002).
7. Fenchel, T. Microbial behavior in a heterogeneous world. *Science* **296**, 1068–1071 (2002).
8. Adler, J. & Dahl, M. A method for measuring the motility of bacteria and for comparing random and non-random motility. *Microbiology* **46**, 161–173 (1967).
9. Ford, R. M., Phillips, B. R., Quinn, J. A. & Lauffenburger, D. A. Measurement of bacterial random motility and chemotaxis coefficients: I. Stopped-flow diffusion chamber assay. *Biotechnol. Bioeng.* **37**, 647–660 (1991).

10. Hol, F. J. H. & Dekker, C. Zooming in to see the bigger picture: microfluidic and nanofabrication tools to study bacteria. *Science* **346**, 1251821 (2014).
11. He, K. & Bauer, C. E. Chemosensory signaling systems that control bacterial survival. *Trends Microbiol.* **22**, 389–398 (2014).
12. Stocker, R. & Seymour, J. R. Ecology and physics of bacterial chemotaxis in the ocean. *Microbiol. Mol. Biol. Rev.* **76**, 792–812 (2012).
13. Garren, M. et al. A bacterial pathogen uses dimethylsulfoniopropionate as a cue to target heat-stressed corals. *ISME J.* **8**, 999–1007 (2014).
14. Lewus, P. & Ford, R. M. Quantification of random motility and chemotaxis bacterial transport coefficients using individual-cell and population-scale assays. *Biotechnol. Bioeng.* **75**, 292–304 (2001).
15. Mesibov, R. & Adler, J. Chemotaxis toward amino acids in *Escherichia coli*. *J. Bacteriol.* **112**, 315–326 (1972).
16. Ahmed, T. & Stocker, R. Experimental verification of the behavioral foundation of bacterial transport parameters using microfluidics. *Biophys. J.* **95**, 4481–4493 (2008).
17. Ammerman, J. W., Fuhrman, J. A., Hagstrom, A. & Azam, F. Bacterioplankton growth in seawater: I. Growth kinetics and cellular characteristics in seawater cultures. *Mar. Ecol. Prog. Ser.* **18**, 31–39 (1984).
18. Taylor, J. R. & Stocker, R. Trade-offs of chemotactic foraging in turbulent water. *Science* **338**, 675–679 (2012).
19. Stocker, R., Seymour, J. R., Samadani, A., Hunt, D. E. & Polz, M. F. Rapid chemotactic response enables marine bacteria to exploit ephemeral microscale nutrient patches. *Proc. Natl Acad. Sci. USA* **105**, 4209–4214 (2008).
20. Azam, F. & Long, R. A. Oceanography: sea snow microcosms. *Nature* **414**, 495–498 (2001).
21. Rinke, C. et al. Validation of picogram- and femtogram-input DNA libraries for microscale metagenomics. *PeerJ* **4**, e2486 (2016).
22. Pedler, B. E., Aluwihare, L. I. & Azam, F. Single bacterial strain capable of significant contribution to carbon cycling in the surface ocean. *Proc. Natl Acad. Sci. USA* **111**, 7202–7207 (2014).
23. Sonnenschein, E. C. et al. Development of a genetic system for *Marinobacter adhaerens* HP15 involved in marine aggregate formation by interacting with diatom cells. *J. Microbiol. Methods* **87**, 176–183 (2011).
24. Kelly, J. R. et al. Measuring the activity of BioBrick promoters using an in vivo reference standard. *J. Biol. Engineer.* https://doi.org/10.1186/1754-1611-3-4 (2017).
25. Temme, K. et al. Modular control of multiple pathways using engineered orthogonal T7 polymerases. *Nucleic Acids Res.* **40**, 8773–8781 (2012).
26. Ahmed, T., Shimizu, T. S. & Stocker, R. Microfluidics for bacterial chemotaxis. *Integ. Biol.* **2**, 604–629 (2010).
27. Marie, D., Partensky, F., Jacquet, S. & Vaulot, D. Enumeration and cell cycle analysis of natural populations of marine picoplankton by flow cytometry using the nucleic acid stain SYBR green I. *Appl. Environ. Microbiol.* **63**, 183–186 (1997).
28. Parks, D. H., Tyson, G. W., Hugenholtz, P. & Beiko, R. G. STAMP: statistical analysis of taxonomic and functional profiles. *Bioinformatics* **30**, 3123–3124 (2014).
29. Langmead, B. & Salzberg, S. L. Fast gapped-read alignment with Bowtie 2. *Nat. Methods* **9**, 357–359 (2012).
30. Li, H. et al. The Sequence Alignment/Map format and SAMtools. *Bioinformatics* **25**, 2078–2079 (2009).

Acknowledgements

The authors thank A. Gavish and A. Vardi for supplying *V. coralliilyticus* YB2, A. Stahl and M. Ullrich for supplying *M. adhaerens* (HP15 ΔfliC) and C. Gao and F. Moser for assistance generating the fluorescent *E. coli* strain used in this study. This work was supported by the Gordon and Betty Moore Foundation through a grant (GBMF3801) to J.S., G.T., P.H. and R.S. J.B.R. was supported by Australian Research Council fellowship DE160100636.

Author contributions

B.S.L., J.-B.R., J.R.S. and R.S. designed the experiments. B.S.L., J.-B.R. and N.S. performed the experiments. B.S.L., J-B.R., V.I.F., F.R. and C.R. analysed the results. C.R., F.R., G.W.T. and P.H. generated and analysed sequencing data. B.S.L., J.-B.R., J.R.S. and R.S. wrote the manuscript. All authors edited the manuscript before submission.

Competing interests

The authors declare no competing financial interests.

Additional information

Supplementary information is available for this paper at doi:10.1038/s41564-017-0010-9.

Reprints and permissions information is available at www.nature.com/reprints.

Correspondence and requests for materials should be addressed to R.S.

Publisher's note: Springer Nature remains neutral with regard to jurisdictional claims inpublished maps and institutional affiliations.

nature research

Corresponding Author: Roman Stocker

Date: Jun 28, 2017

Life Sciences Reporting Summary

Nature Research wishes to improve the reproducibility of the work we publish. This form is published with all life science papers and is intended to promote consistency and transparency in reporting. All life sciences submissions use this form; while some list items might not apply to an individual manuscript, all fields must be completed for clarity.

For further information on the points included in this form, see Reporting Life Sciences Research. For further information on Nature Research policies, including our data availability policy, see Authors & Referees and the Editorial Policy Checklist.

Experimental design

1. Sample size

   Describe how sample size was determined. The sample size was based on pilot studies.

2. Data exclusions

   Describe any data exclusions. No data was excluded.

3. Replication

   Describe whether the experimental findings were reliably reproduced. Number of replicates was based on pilot studies.

4. Randomization

   Describe how samples/organisms/participants were allocated into experimental groups. Within the device, the chemoattractants were always placed in a row together, but the location of that row was randomized in each device. This was done to limit any effects geometry may play.

5. Blinding

   Describe whether the investigators were blinded to group allocation during data collection and/or analysis. No blinding was carried out.

   Note: all studies involving animals and/or human research participants must disclose whether blinding and randomization were used.

6. Statistical parameters

   For all figures and tables that use statistical methods, confirm that the following items are present in relevant figure legends (or the Methods section if additional space is needed).

n/a	Confirmed	
☐	☒	The exact sample size (*n*) for each experimental group/condition, given as a discrete number and unit of measurement (animals, litters, cultures, etc.)
☐	☒	A description of how samples were collected, noting whether measurements were taken from distinct samples or whether the same sample was measured repeatedly.
☒	☐	A statement indicating how many times each experiment was replicated
☐	☒	The statistical test(s) used and whether they are one- or two-sided (note: only common tests should be described solely by name; more complex techniques should be described in the Methods section)
☒	☐	A description of any assumptions or corrections, such as an adjustment for multiple comparisons
☐	☒	The test results (e.g. *p* values) given as exact values whenever possible and with confidence intervals noted
☐	☒	A summary of the descriptive statistics, including central tendency (e.g. median, mean) and variation (e.g. standard deviation, interquartile range)
☐	☒	Clearly defined error bars

See the web collection on statistics for biologists for further resources and guidance.

Software

Policy information about availability of computer code

7. Software

   Describe the software used to analyze the data in this study. All analysis was carried out using the standard MATLAB image processing

toolkit.

For all studies, we encourage code deposition in a community repository (e.g. GitHub). Authors must make computer code available to editors and reviewers upon request. The *Nature Methods* guidance for providing algorithms and software for publication may be useful for any submission.

Materials and reagents

Policy information about availability of materials

8. Materials availability

Indicate whether there are restrictions on availability of unique materials or if these materials are only available for distribution by a for-profit company.	All materials should be openly available.

9. Antibodies

Describe the antibodies used and how they were validated for use in the system under study (i.e. assay and species).	N/A.

10. Eukaryotic cell lines

a. State the source of each eukaryotic cell line used.	N/A.
b. Describe the method of cell line authentication used.	N/A.
c. Report whether the cell lines were tested for mycoplasma contamination.	N/A.
d. If any of the cell lines used in the paper are listed in the database of commonly misidentified cell lines maintained by ICLAC, provide a scientific rationale for their use.	N/A.

Animals and human research participants

Policy information about studies involving animals; when reporting animal research, follow the ARRIVE guidelines

11. Description of research animals

Provide details on animals and/or animal-derived materials used in the study.	N/A.

Policy information about studies involving human research participants

12. Description of human research participants

Describe the covariate-relevant population characteristics of the human research participants.	N/A.